ISBN: 978-3-95450-247-9 ISSN: 2673-5490 doi: 10.18429/JACoW-IPAC2024-WEPG21

UPDATES ON THE CORNELL CRYO-MTE-METER BEAMLINE *

Charles Zhang†, Adam Bartnik, Elena Echeverria, Abigail Flint, Chad Pennington, Jared Maxson
Cornell Laboratory for Accelerator-Based Sciences and Education, Ithaca, NY, United States
Alice Galdi, University of Salerno, Fisciano, SA, Italy
William Li, Brookhaven National Laboratory, Upton, NY, United States
Chris Pierce, University of Chicago, Chicago, IL, United States

Abstract

A critical factor in determining the limit of the brightness of an electron beam is the mean transverse energy (MTE) of its source, which describes the spread in transverse momentum of electrons at the moment of emission from the source. To increase beam brightness, there has been much work in growing novel photocathodes with low MTE and high quantum efficiency (QE) near threshold photoemission excitation energies. Therefore, it is important to have a testing platform for accurately measuring the MTE of a cathode over a range of cryogenic temperatures and photoexcitation energies, with self-consistent results across multiple measurement techniques. Here, we will discuss the characterization and operation of the Cornell Cryo-MTE-Meter beamline which aims to fulfill these criteria for a robust photocathode testing platform.

INTRODUCTION

The need for brighter electron beams in applications such as free electron lasers and ultrafast electron microscopy [1,2] requires advances in electron sources. One particular avenue for achieving brighter beams is developing photocathodes with smaller transverse momentum spread, which is directly proportional to a figure of merit known as the mean transverse energy (MTE). The MTE is often obtained by first measuring the 2D or 4D transverse beam emittance in a dedicated diagnostic after an emittance preserving transport section. The MTE is directly related to the normalized beam emittance by,

$$\epsilon_n = \sigma_x \sqrt{\frac{\mathrm{MTE}}{m_e c^2}}, \tag{1}$$

where σ_x is the initial rms beam spot size on the cathode, typically inferred from the photoexcitation laser spot size. Here, we define the normalized 4D transverse emittance as,

$$\epsilon_n = \frac{1}{m_e c} \begin{vmatrix} \langle x^2 \rangle & \langle x p_x \rangle & \langle xy \rangle & \langle x p_y \rangle \\ \langle x p_x \rangle & \langle p_x^2 \rangle & \langle y p_x \rangle & \langle p_x p_y \rangle \\ \langle xy \rangle & \langle y p_x \rangle & \langle y^2 \rangle & \langle y p_y \rangle \\ \langle x p_y \rangle & \langle p_x p_y \rangle & \langle y p_y \rangle & \langle p_y^2 \rangle \end{vmatrix}^{1/4}, \tag{2}$$

where x and y are the transverse coordinates. There are a variety of methods to measure the beam emittance [3, 4], but here we will mainly focus on solenoid scans and 4D phase space scans. Since the underlying assumption for these methods is the preservation of beam emittance through transport, we will present a characterization of the beamline transport that confirms this, as well as discuss additional errors present in the environment.

THE BEAMLINE

In the Cryo-MTE-Meter beamline, a DC photogun accelerates electrons from an alkali-antimonide photocathode to 15 keV. The photocathode is continuously driven by a 532 nm diode laser that is passed through a pinhole, which is imaged onto the cathode, resulting in a round flat-top profile with variable diameter (50, 70, 100 μm rms). Upon exiting the gun, the beam is focused by a solenoid onto either the detector when performing solenoid scans or a removable aperture with varying diameters (30, 50, 70 μm) when performing 4D phase space imaging. Simultaneously, a pair of normal and skew quadrupole corrector magnets, built into the solenoid, are manually tuned to correct for stray quadrupole fields. Dipole corrector magnets steer the beam onto the detector when performing solenoid scans or scans it across the aperture when performing 4D phase space scans. The detector consists of a microchannel plate followed by a scintillator screen, which is imaged by a scientific CMOS camera.

BEAMLINE CHARACTERIZATION

Linear Transport

One of the causes of emittance growth are the various aberrations in the beamline optics, which appear as nonlinear transformations distorting the beam phase space distribution. Removing these aberrations is nearly impossible, so it is essential to determine the proper initial beam conditions to minimize emittance growth. We perform a 2D pincushion scan, shown in Fig. 1, of the photoexcitation laser within a 400 μm by 400 μm region on the photocathode and simultaneously measure the position of the beam centroid on the detector. We find a roughly 200 μm by 400 μm region on the cathode that can be related to the corresponding region on the detector by a linear transformation, thus indicating the initial beam positions on the cathode where the emittance will be preserved throughout the beam transport.

Quadrupole Field Correction

Stray quadrupole fields in the beamline will introduce coupling between the transverse axes of motion. This poses

* This work was supported by the U.S. National Science Foundation under Award PHY-1549132, the Center for Bright Beams, and DOE grant awards DE-AC02-76SF00515 and DE-SC0020144.
† cz266@cornell.edu

15th International Particle Accelerator Conference,Nashville, TN JACoW Publishing
ISBN: 978-3-95450-247-9 ISSN: 2673-5490 doi: 10.18429/JACoW-IPAC2024-WEPG21

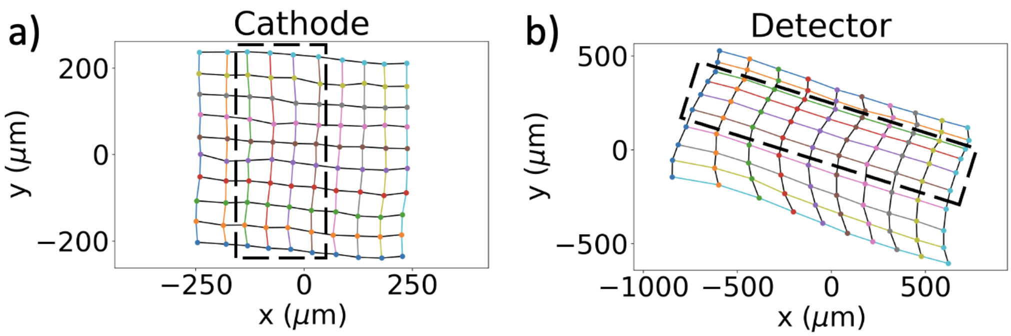

Figure 1: Pincushion scans: (a) initial beam position at the cathode, (b) final beam position at the detector, with corresponding initial and final positions matched by color. The region enclosed by the black dashed lines indicates the initial position on the cathode for which the beam undergoes approximately linear transport and preserves emittance through the beamline.

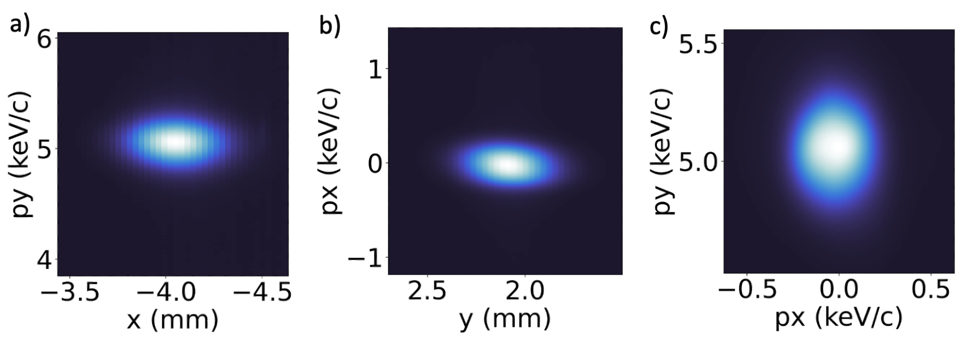

Figure 2: Example of (a) x-p_y, (b) y-p_y, and (c) p_x-p_y phase space projections of the measured 4D phase space that show minimal correlation.

a significant problem since the calculation of emittance from solenoid scans often assumes no transverse coupling. To account for this during measurement, we manually tune quadrupole correctors to eliminate beam tilt and symmetrize the beam as observed at the detector. Confirming this further, the measured phase space of the beam also shows zero x-p_y, y-p_y, and p_x-p_y correlation as shown in Fig 2.

Solenoid Centering

Due to variations in the cathode transfer process, drift in the laser optics, and other factors, the beam may be offset from the center upon exiting the gun and travel through aberrations within the solenoid, leading to emittance growth. To minimize the effects of any potential misalignment, for every new cathode, we vary the solenoid current while manually adjusting the laser position on the cathode to minimize the movement of the beam at the detector. This process is repeated until the range of motion of the beam is comparable to the jitter caused by noise in the system.

Miscellaneous Errors

The resolution of the beam images is limited by the point spread function intrinsic to the microchannel plate detector. To characterize the point spread function, we passed the beam through the smallest aperture available, which is around 30 μm, and tuned the solenoid until the minimum beam size at the detector was achieved. This turned out to be roughly 80 μm rms, or 0.16 mrad in terms of phase space angular resolution. We can calculate the minimum emittance and MTE measurable by 4D phase space imaging in this setup using General Particle Tracer simulations, with the initial beam size of 50 μm rms at the cathode, as determined by the smallest laser spot size, and zero initial MTE. In simulation, the beam is focused at the aperture, where the aperture size of 30 μm is added in quadrature to the rms beam size there and similarly for the rms beam angular spread with the detector resolution of 0.16 mrad. From Eq. (2), we find that the smallest measurable emittance and MTE is roughly 1.5 nm and 0.5 meV respectively.

METHODS

Here we focus on two methods for measuring emittance, solenoid scans and 4D phase space scans. Emittance was measured for each laser spot size using both methods. The photocathode used for all measurements shown here was K-Sb grown on niobium at room temperature, with typical beam currents ranging within 0.5 - 1 nA.

Solenoid Scan

The beam is imaged at the detector while the solenoid current is varied such that the beam size crosses the waist. At each solenoid current, a background image is taken with the beam steered offscreen and the rms beam size in both transverse directions is calculated from a supergaussian fit of

15th International Particle Accelerator Conference,Nashville, TN JACoW Publishing
ISBN: 978-3-95450-247-9 ISSN: 2673-5490 doi: 10.18429/JACoW-IPAC2024-WEPG21

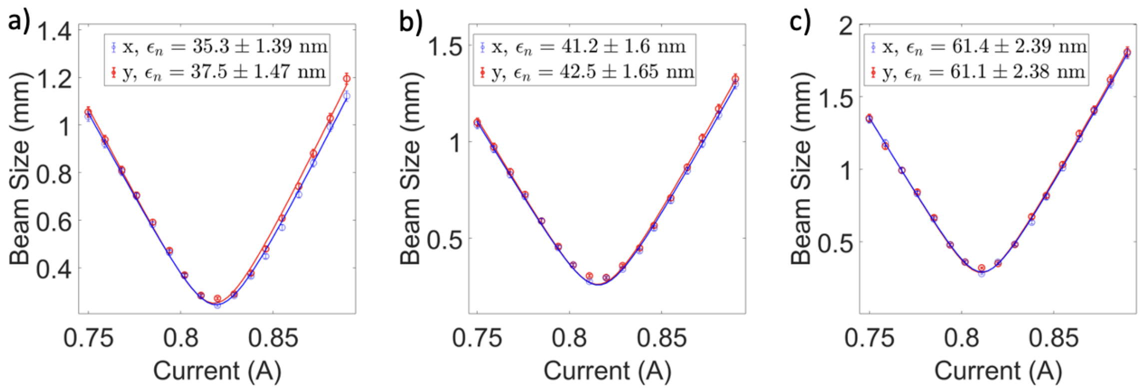

Figure 3: Beam size vs. solenoid current and fits based on the transfer matrix using laser spot sizes of (a) 50, (b) 70, and (c) 100 µm rms.

the beam image with the background subtracted. An example of a full set of solenoid scans is shown in Fig. 3, where effects of the quadrupole field correction can also be seen in the close agreement between the 'x' and 'y' beam sizes. From known electromagnetic fieldmaps of the beamline elements, we calculate 2D linear transfer matrices $\mathbf{R}_i$ for all solenoid currents using the methods described in Ref. [5]. The beam sizes vs solenoid current data is fitted to $\mathbf{R}^2_{11,i}\sigma_x^2 + \mathbf{R}^2_{12,i}\sigma_{px}^2 = \sigma_{x,i}^2$, where σ_x and σ_{px} are the initial beam sizes in position and momentum and $\sigma_{x,i}$ is the beam size measured for the ith data point. Assuming zero correlation between the position and momentum at the surface of the photocathode, as well as no coupling between the transverse directions, the covariance matrix in Eq. 2 is purely diagonal and the 4D emittance is simply $\epsilon_n = \sqrt{\sigma_x\sigma_{px}\sigma_y\sigma_{py}}/(m_e c)$. The error of the emittance is propagated from the beam size uncertainty using a Monte Carlo method.

4D Phase Space Imaging

A dipole corrector magnet scans the beam across the aperture in both transverse directions. The transmitted beamlet expands in a drift section of known length and is steered back onto the detector using another dipole corrector magnet, which is left unchanged during the scan. Since the drift length is known, the beamlet image can be used to generate its angular distribution, which is directly related to its momentum distribution by a factor of $\gamma\beta m_e c$. With the beamlet's momentum distribution being imaged at each scan position, a 4D phase space can be constructed. To obtain the covariance matrix in Eq. (2), the 4D phase space is projected into 2-dimensions for each pair of (x, px, y, py) coordinates and fitted by a rotated supergaussian. To handle noise in the phase space, the supergaussian includes a constant background term that is subtracted, after which the beam moments and correlations are computed from the supergaussian fit. Each 2D phase space yields elements of the covariance matrix and the 4D emittance can then be obtained from Eq. (2). The error of the 4D emittance is propagated from the uncertainty of the supergaussian fits to the 2D phase spaces using a Monte Carlo method.

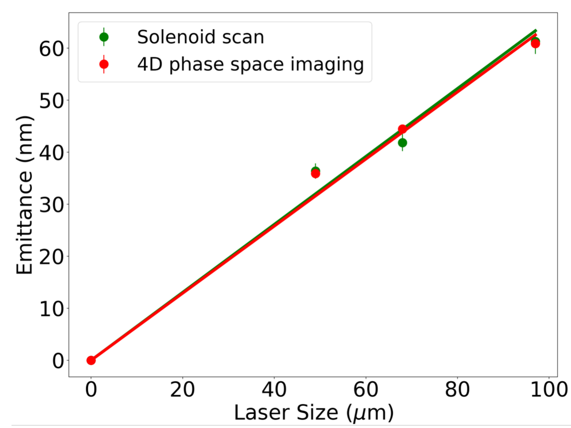

Figure 4: Emittance vs. rms laser spot size measured by solenoid scans and 4D phase space imaging.

RESULTS

The 4D emittances measured by solenoid scan and 4D phase space imaging at each laser spot size is shown in Fig. 4. Linear fits of the 4D emittance to the laser spot size, as per Eq. (1), yield MTE of 212 ± 3 meV from the 4D phase space imaging and 218 ± 10 meV from the solenoid scan. The emittances and MTEs acquired through both methods are in good agreement.

CONCLUSION

By performing characterization of beamline aberrations and correction of higher-order stray fields, we demonstrate self-consistent measurement of MTE of an alkali-antimonide photocathode using solenoid scan and 4D phase space imaging. This characterization and tuning of the beamline will also allow us to directly measure the initial momentum space [6] at the cathode, which will ultimately yield the full 4D transfer matrix of the beamline. With the assurance that the Cryo-MTE-Meter can reliably measure MTE, we plan on measuring the MTE of photocathodes at cold temperatures and with a variety of photoexcitation energies.

ISBN: 978-3-95450-247-9 ISSN: 2673-5490 doi: 10.18429/JACoW-IPAC2024-WEPG21

REFERENCES

[1] J. B. Rosenzweig *et al.*, “Next generation high brightness electron beams from ultrahigh field cryogenic rf photocathode sources,”*Phys. Rev. Accel. Beams*, vol. 22, no. 2, p. 023403, Feb. 2019. doi:10.1103/physrevaccelbeams.22.023403

[2] W. H. Li *et al.*, “A kiloelectron-volt ultrafast electron microdiffraction apparatus using low emittance semiconductor photocathodes,”*Earthquake Eng. Struct. Dyn.*, vol. 9, no. 2, p. 024302, Mar. 2022. doi:10.1063/4.0000138

[3] H. Lee, S. Karkare, L. Cultrera, A. Kim, and I. V. Bazarov, “Review and demonstration of ultra-low-emittance photocathode measurements,”*Rev. Sci. Instrum.*, vol. 86, no. 7, p. 073309, Jul. 2015. doi:10.1063/1.4927381

[4] M. Gordon *et al.*, “Four-dimensional emittance measurements of ultrafast electron diffraction optics corrected up to sextupole order,”*Phys. Rev. Accel. Beams*, vol. 25, no. 8, p. 084001, Aug. 2022. doi:10.1103/physrevaccelbeams.25.084001

[5] C. Gulliford and I. Bazarov, “New method for generating linear transfer matrices through combined rf and solenoid fields,”Physical Review Special Topics - Accelerators and Beams, vol. 15, no. 2, p. 024002, Feb. 2012. doi:10.1103/physrevstab.15.024002

[6] C. Zhang, A. Bartnik, C. Pennington, E. Echeverria, and J. Maxson, “Reconstructing 4D source momentum space via aperture scans”, in *Proc. IPAC’23*, Venice, Italy, May 2023, pp. 4595–4597. doi:10.18429/JACoW-IPAC2023-THPL071